

*Article*

# The truncated lognormal distribution as a luminosity function for SWIFT-BAT gamma-ray bursts

Lorenzo Zaninetti <sup>1</sup>,<sup>1</sup> Physics Department, via P.Giuria 1,  
I-10125 Turin, Italy*Version April 24, 2022 submitted to Galaxies. Typeset by L<sup>A</sup>T<sub>E</sub>X using class file mdpi.cls*

---

**Abstract:** The determination of the luminosity function (LF) in gamma ray bursts (GRBs) depends on the adopted cosmology, each one characterized by its corresponding luminosity distance. Here we analyse three cosmologies: the standard cosmology, the plasma cosmology, and the pseudo-Euclidean universe. The LF of the GRBs is firstly modeled by the lognormal distribution and the four broken power law, and secondly by a truncated lognormal distribution. The truncated lognormal distribution fits acceptably the range in luminosity of GRBs as a function of the redshift.

**Keywords:** Cosmology; Observational cosmology; Distances, redshifts, radial velocities, spatial distribution of galaxies;

**PACS classifications:** 98.80.-k ; 98.80.Es 98.62.Py ;

---

## 1. Introduction

The number of gamma ray bursts (GRBs) for which we know the redshift and the flux is 760, according to the SWIFT-BAT catalog of [1], available at the Centre de Données Astronomiques de Strasbourg (CDS), with the name *J/ApJS/207/19*. The above catalog gives the hard X-ray flux, the spectral index, the redshift, and the X-ray luminosity. The luminosity data of this catalog, which is a theoretical evaluation, is given in the framework of the  $\Lambda$ CDM cosmology with  $H_0 = 70 \text{ km s}^{-1} \text{ Mpc}^{-1}$ ,  $\Omega_M = 0.3$  and  $\Omega_\Lambda = 0.7$ . A calibration and a comparison can be done with the models for luminosity here implemented. This large number of observed objects allows applying different cosmologies in order to find the luminosity and the luminosity function (LF) for GRBs. At the moment of writing, the standard

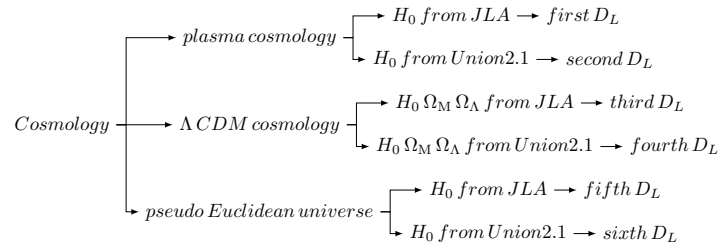


**Figure 1.** Flowchart for the luminosity distances here analysed.

20 cosmology is the  $\Lambda$ CDM cosmology, but other cosmologies such as the plasma or the pseudo-Euclidean  
 21 cosmology can also be analysed. Once the luminosity is obtained, we can model the LF by adopting the  
 22 lognormal distribution, see [2,3] and by a four broken power law.

23 In the hypothesis that the luminosity of a GRB is due to the early phase of a supernova (SN), the  
 24 minimum and maximum are due to the various parameters which drive the SN's light curve, see [4].

## 25 2. Preliminaries

26 This section analyses the luminosity in the  $\Lambda$ CDM cosmology, in the plasma cosmology and in the  
 27 pseudo-Euclidean cosmology. Careful attention should be paid to the multiplicative effects of the main  
 28 models (3) for the empirical catalogs of SNs (2), which means 6 different cases to be analysed, see Figure  
 29 1.

### 30 2.1. Observed luminosity

In the framework of the standard cosmology, the received flux,  $f$ , is

$$f = \frac{L}{4\pi D_L(z)^2} \quad , \quad (1)$$

where  $D_L(z)$  is the luminosity distance, which depends on the parameters of the adopted cosmological model and  $z$  is the redshift. As a consequence, the luminosity is

$$L = 4\pi D_L(z)^2 f \quad . \quad (2)$$

The above formula is then corrected by a  $k$ -correction,  $k(z, \gamma)$ , where

$$k(z, \gamma) = \frac{\int_{1\text{keV}}^{10^4\text{keV}} C E'^{-\gamma} E' dE'}{\int_{15(1+z)\text{keV}}^{150(1+z)\text{keV}} C E'^{-\gamma} E' dE'} \quad , \quad (3)$$

where  $C$  is a constant and  $\gamma$  is the observed spectral index in energy, see [5] for more details. The corrected luminosity is therefore

$$L = 4\pi D_L(z)^2 f k(z, \gamma) \quad . \quad (4)$$

31 In the case of the survey from the 70 month SWIFT-BAT, the flux  $f$  is given in  $\frac{fW}{m^2}$ ,  $\gamma$  and  $z$  are positive  
 32 numbers, see [1]; Table 1 reports a test-GRB.

**Table 1.** Test GRB

SWIFT name	flux in $\frac{fW}{m^2}$	$\gamma$	z	$\log(L(\text{erg s}^{-1}))$
J0017.1+8134	10.12	2.53	3.3660	48.01

### 33 2.2. Luminosity in the standard cosmology

34 The luminosity distance,  $D_L$ , in the  $\Lambda$ CDM cosmology can be expressed in terms of a Padé  
 35 approximant, once we provide the Hubble constant,  $H_0$ , expressed in  $\text{km s}^{-1} \text{Mpc}^{-1}$ , the velocity of  
 36 light,  $c$ , expressed in  $\text{km s}^{-1}$ , and the three numbers  $\Omega_M$ ,  $\Omega_K$ , and  $\Omega_\Lambda$ , see [6] for more details or Table  
 2.

**Table 2.** Numerical values of the  $\Lambda$ CDM cosmology.

compilation	$H_0$ in $\text{km s}^{-1} \text{Mpc}^{-1}$	$\Omega_M$	$\Omega_\Lambda$
Union 2.1	69.81	0.239	0.651
JLA	69.398	0.181	0.538

37

A further application of the minimax rational approximation, which is characterized by the two  
 parameters  $p$  and  $q$ , allows finding a simplified expression for the luminosity distance, see eqns (33a)  
 and (33b) in [6]. The above minimax approximation when  $p = 3, q = 2$  is

$$D_{L,3,2} = \frac{p_0 + p_1 z + p_2 z^2 + p_3 z^3}{q_0 + q_1 z + q_2 z^2} \text{Mpc} \quad , \quad (5)$$

38 and Table 3 reports the coefficients for the two compilations here used.

**Table 3.** Numerical values of the 7 coefficients of the minimax approximation for the Union 2.1 compilation and the JLA compilation.

Coefficient	Union 2.1	JLA
$p_0$	0.3597252600	0.4429883062
$p_1$	5.612031882	6.355991909
$p_2$	5.627811123	5.405310650
$p_3$	0.05479466285	0.04413321265
$q_0$	0.010587821	0.0129850304
$q_1$	0.1375418627	0.1546989174
$q_2$	0.1159043801	0.1097492834

The monochromatic luminosity, X-band (14–195 keV), without  $k-z$  correction,  $\log(L_{3,2})_b$  according to eqn (2) is

$$\log(L_{3,2}(\text{erg s}^{-1}))_b = 0.43429 \ln \left( 1.1964 \frac{\text{fluxfwm2} (16.6843 + (194.6669 + (1878.8341 + 180.34010 z) z) z)^2}{(0.08644 + (0.2578 - 0.00849 z) z)^2} \right) + 38.0 \quad \text{Union 2.1} \quad . \quad (6)$$

In the case of a test-GRB with parameters as in Table 1, the above formula gives  $\log(L) = 48.13$  against  $\log(L_{\text{SWIFT}}) = 48.01$  of the SWIFT-BAT catalog. The goodness of the approximation is evaluated through the percentage error,  $\eta$ , which is

$$\eta = \frac{|\log(L_{3,2}(\text{erg s}^{-1}))_b - \log(L_{\text{SWIFT}})|}{\log(L_{\text{SWIFT}})} \times 100 \quad , \quad (7)$$

and over all the elements of the SWIFT-BAT catalog  $2.28 \cdot 10^{-5} \% \leq \eta \leq 0.295\%$ . We now report an expression for the luminosity of a GRB, eqn (4), based on the minimax approximation when the Union 2.1 compilation is considered

$$\log(L_{3,2}(\text{erg s}^{-1})) = 41.5647 + 0.4342 \ln \left( 32522 \frac{\text{fluxfwm2} (z + 10.3144)^2 (z^2 + 0.10378 z + 0.0089695)^2}{(-0.08644 - 0.2578 z + 0.008491 z^2)^2} \right) + \left( \frac{-1 + 0.5 \gamma}{(1 + z)^2 ((15 + 15 z)^{-\gamma} - 100 (150 + 150 z)^{-\gamma})} \right) \text{Union 2.1} \quad , \quad (8)$$

39 where fluxfwm2 is the flux expressed in  $\frac{fW}{m^2}$ .

In the case of a test-GRB with parameters as in Table 1, the above formula gives  $\log(L) = 54.512$  which means a bigger luminosity of  $\approx 6$  decades with respect to the band luminosity. Figure 2 reports the luminosity–redshift distribution for the SWIFT-BAT survey as well a theoretical lower curve which can be found by inserting the minimum flux in eqn (8). Another useful quantity is the angular diameter distance,  $D_A$ , which is

$$D_A = \frac{D_L}{(1 + z)^2} \quad , \quad (9)$$

see [7], and therefore

$$D_{A,3,2} = \frac{D_{L,3,2}}{(1 + z)^2} \quad . \quad (10)$$

### 40 2.3. Luminosity in the plasma cosmology

The distance  $d$  in the plasma cosmology has the following dependence:

$$d(z) = \frac{\ln(z + 1) c}{H_0} \quad , \quad (11)$$

see [8–11] and Table 4. The monochromatic luminosity, X-band (14–195 keV), is

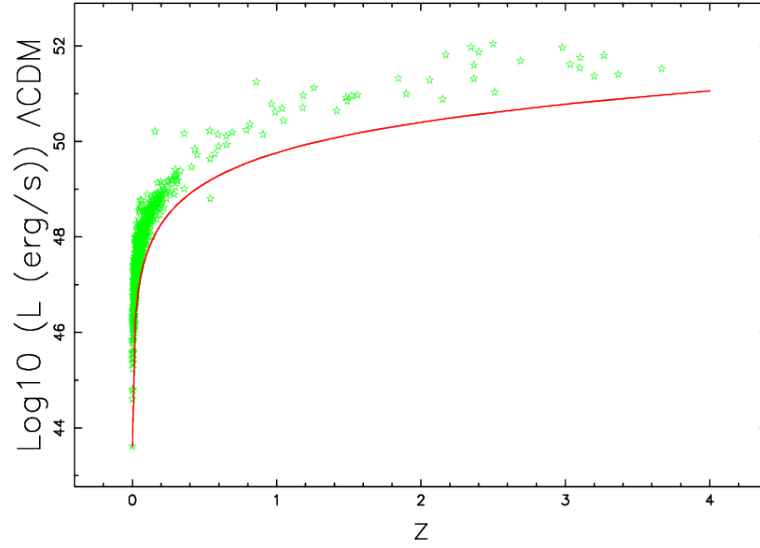


**Figure 2.** Luminosity in the  $\Lambda$ CDM cosmology versus redshift for 784 GRB as given by the 70 month SWIFT-BAT survey (green points) and theoretical curve for the lowest luminosity at a given redshift (red curve), see eqn (8).

**Table 4.** Numerical values of  $H_0$  in  $\text{km s}^{-1} \text{Mpc}^{-1}$  (plasma cosmology) for the Union 2.1 compilation and the JLA compilation.

Union 2.1	JLA
$H_0 = 74.2 \pm 0.24$	$H_0 = 74.45 \pm 0.2$

$$\log(L(z)) = \frac{\ln(19531902.82 \text{ fluxfw}2 (\ln(1+z))^2)}{\ln(10)} + 38 \quad . \quad (12)$$

41 In the case of a test-GRB with parameters as in Table 1, the above formula gives  $\log(L) = 46.63$ , which  
 42 a lower value than the  $\log(L_{\text{SWIFT}}) = 48.01$  of the SWIFT-BAT catalog.

The luminosity in the case of the absence of absorption is

$$L(z) = 4\pi d(z)^2 f k(\gamma) \quad , \quad (13)$$

where the  $k(\gamma)$  correction is

$$k(\gamma) = \frac{\int_{1\text{keV}}^{10^4\text{keV}} C E'^{-\gamma} E' dE'}{\int_{15\text{keV}}^{150\text{keV}} C E'^{-\gamma} E' dE'} \quad . \quad (14)$$

43 There is no relativistic correction in the denominator because the plasma cosmology is both static and  
 44 Euclidean. Figure 3 reports the luminosity in the plasma cosmology as a function of the redshift as well  
 45 as the theoretical luminosity.

#### 46 2.4. Luminosity in the pseudo-Euclidean cosmology

The distance  $d$  in the pseudo-Euclidean cosmology has the following dependence:

$$d(z) = \frac{zc}{H_0} \quad , \quad (15)$$

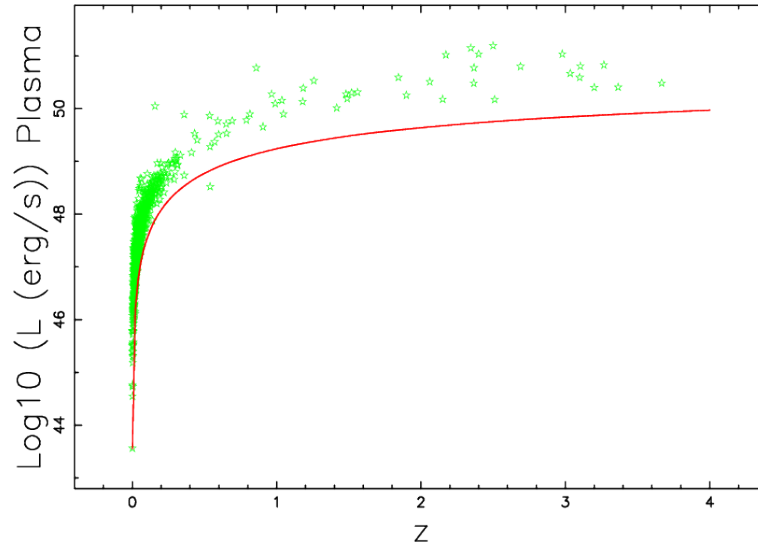


**Figure 3.** Luminosity in the plasma cosmology versus redshift for 784 GRB as given by the 70 month SWIFT-BAT survey (green points) and theoretical curve for the lowest luminosity at a given redshift (red curve), see eqn (14).

and we used  $H_0 = 67.93 \text{ km s}^{-1} \text{ Mpc}^{-1}$ , see Table 5.

**Table 5.** Numerical values of  $H_0$  in  $\text{km s}^{-1} \text{ Mpc}^{-1}$  (pseudo-Euclidean cosmology) for the Union 2.1 compilation and the JLA compilation when the redshift covers the range  $[0, 0.1]$

Union 2.1	JLA
$H_0 = 67.93 \pm 0.38$	$H_0 = 67.51 \pm 0.42$

47

The above formula gives approximate results up to  $z \ll 1.0$ . The monochromatic luminosity, X-band (14–195 keV), is

$$L(z) = 4\pi d(z)^2 f \quad , \quad (16)$$

where the  $k(z)$  correction is absent or

$$\log(L(z)) = \frac{\ln(19531902.82 \text{ fluxfw} z^2)}{\ln(10)} + 38 \quad . \quad (17)$$

#### 48 2.5. High versus low $z$

The differences between the four distances here used, which are the luminosity distance and the angular-diameter distance in the  $\Lambda$ CDM, the plasma cosmology distance, and the pseudo-Euclidean cosmology distance, can be outlined in terms of a percentage difference,  $\Delta$ . As an example for  $D_A$ ,

$$\Delta = \frac{|D_L(z) - D_A(z)|}{D_L(z)} \times 100 \quad . \quad (18)$$

49 Figure 4 reports the four distances and for  $z \leq 0.05$  the three percentage differences are lower than  
50 10%. In the framework of the two Euclidean distances, the plasma and the pseudo-Euclidean one, for

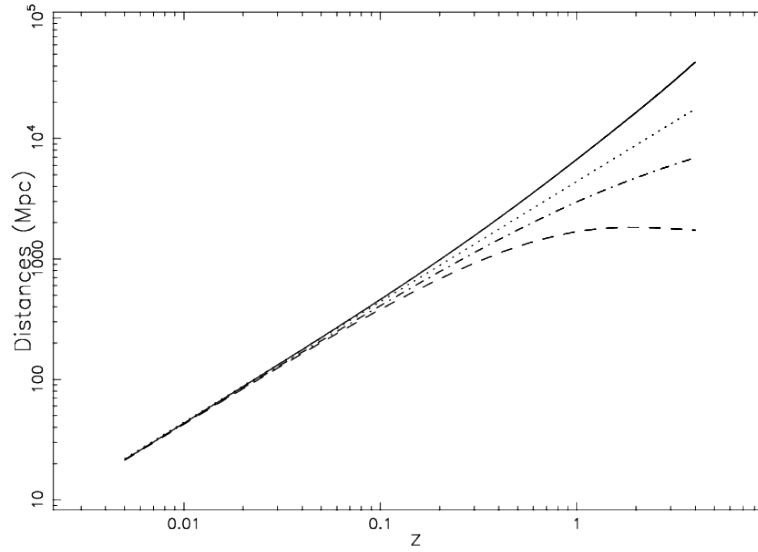


**Figure 4.** The distances here adopted: luminosity distance,  $D_L$ , in  $\Lambda$ CDM (full line), angular-diameter distance,  $D_A$ , in  $\Lambda$ CDM (dash line), plasma cosmology distance,  $d$ , (dot-dash-dot-dash line) and pseudo-Euclidean cosmology distance (dotted line).

51  $z \leq 0.15$  the percentage difference is lower than 10%. Therefore the boundary between low and high  $z$   
 52 can be fixed at  $z = 0.05$ .

### 53 3. Two existing distributions

54 This section reviews the four broken power law distribution and the lognormal distribution and derives  
 55 an analytical expression for the number of GRBs for a given flux in the linear and non-linear cases.

#### 56 3.1. The four broken power law distribution

The four broken power law has the following piecewise dependence:

$$p(L) \propto L^{\alpha_i} \quad , \quad (19)$$

each of the four zones being characterized by a different exponent  $\alpha_i$ . In order to have a PDF normalized to unity, one must have

$$\sum_{i=1,4} \int_{L_i}^{L_{i+1}} c_i L^{\alpha_i} dL = 1 \quad . \quad (20)$$

For example, we start with  $c_1=1$ :  $c_2$  will be determined by the following equation:

$$c_1(L_2 - \epsilon)^{\alpha_1} = c_2(L_2 + \epsilon)^{\alpha_2} \quad , \quad (21)$$

57 where  $\epsilon$  is a small number, e.g.  $\epsilon = \frac{L_2}{10^{+8}}$ . This PDF is characterized by 9 parameters and takes values  $L$   
 58 in the interval  $[L_1, L_5]$ .

59 *3.2. Lognormal distribution*

Let  $L$  be a random variable taking values  $L$  in the interval  $[0, \infty]$ ; the *lognormal* probability density function (PDF), following [12] or formula (14.2)' in [13], is

$$PDF(L; L^*, \sigma) = \frac{\sqrt{2} e^{-\frac{1}{2} \frac{1}{\sigma^2} (\ln(\frac{L}{L^*}))^2}}{2 L \sigma \sqrt{\pi}} \quad , \quad (22)$$

where  $L^* = \exp \mu_{LN}$  and  $\mu_{LN} = \ln L^*$ . The mean luminosity is

$$E(L; L^*, \sigma) = L^* e^{\frac{1}{2} \sigma^2} \quad , \quad (23)$$

and the variance,  $Var$ , is

$$Var(L^*, \sigma) = e^{\sigma^2} (-1 + e^{\sigma^2}) L^{*2} \quad . \quad (24)$$

The distribution function (DF) is

$$DF(L; L^*, \sigma) = \frac{1}{2} + \frac{1}{2} \operatorname{erf} \left( \frac{1}{2} \frac{\sqrt{2} (\ln(L) - \ln(L^*))}{\sigma} \right) \quad , \quad (25)$$

where  $\operatorname{erf}(z)$  is the error function, see [14]. A luminosity function for GRB,  $PDF_{GRB}$ , can be obtained by multiplying the lognormal PDF by  $\Phi^*$ , which is the number of GRB per unit volume,  $\text{Mpc}^3$  units for unit time, yr units,

$$\Phi(L; L^*, \sigma) = \Phi^* \frac{\sqrt{2} e^{-\frac{1}{2} \frac{1}{\sigma^2} (\ln(\frac{L}{L^*}))^2}}{2 L \sigma \sqrt{\pi}} \frac{\text{number}}{\text{Mpc}^3 \text{ yr}} \quad . \quad (26)$$

A numerical value for the constant  $\Phi^*$  can be obtained by dividing the number of GRB,  $N_{GRB}$ , observed in a time,  $T$ , in a given volume  $V$  by the volume itself and by  $T$ , which is the time over which the phenomena are observed, in the case of SWIFT-BAT, 70 month, see [1],

$$\Phi^* = \frac{N_{GRB}}{V T} \text{Mpc}^{-3} \text{yr}^{-1} \quad , \quad (27)$$

where the volume is different in the three cosmologies,

$$V = \frac{4}{3} \pi \left( \frac{cz}{H_0} \right)^3 \text{Mpc}^3 \quad \text{pseudo - Euclidean cosmology} \quad (28a)$$

$$V = \frac{4}{3} \pi \left( \frac{\ln(z+1)c}{H_0} \right)^3 \text{Mpc}^3 \quad \text{plasma cosmology} \quad (28b)$$

$$V = \frac{4}{3} \pi (D_{A,3,2})^3 \text{Mpc}^3 \quad \Lambda \text{CDM cosmology} \quad , \quad (28c)$$

60 where  $D_{A,3,2}$  has been defined in eqn (10). The parameters of the fit for the four broken power law's  
61 PDF are reported in Table 6 when the luminosity is taken with the  $k(z)$  correction, Figure 5.

62 The parameters of the fit for the lognormal PDF are reported in Table 7 when the luminosity is taken  
63 with the  $k(z)$  correction.

64 The case of LF modeled by a lognormal PDF with  $L$  as represented by a monochromatic luminosity  
65 in the X-band (14–195 keV) is reported in Table 8.

66 The goodness of the fit with the lognormal PDF has been assessed by applying the  
67 Kolmogorov–Smirnov (K–S) test [15–17]. The K–S test, as implemented by the FORTRAN subroutine



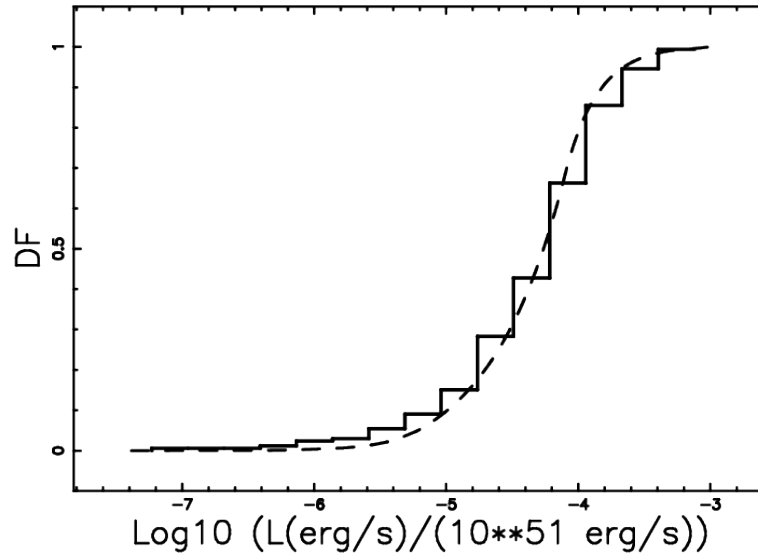


**Figure 5.** Observed DF (step-diagram) for GRB luminosity and superposition of the four broken power laws' DFs (line), case of  $\Lambda$ CDM cosmology with parameters as in Table 6.

**Table 6.** The 9 parameters of the four broken power laws for the  $\Lambda$ CDM cosmology where eqn (8) was used and the two parameters of the K–S test  $D$  and  $P_{KS}$ .

Name	
$L_1$ in $\frac{L^*}{10^{51} \text{erg s}^{-1}}$	$4 \cdot 10^{-8}$
$L_2$ in $\frac{L^*}{10^{51} \text{erg s}^{-1}}$	$5 \cdot 10^{-7}$
$L_3$ in $\frac{L^*}{10^{51} \text{erg s}^{-1}}$	$6.3 \cdot 10^{-6}$
$L_4$ in $\frac{L^*}{10^{51} \text{erg s}^{-1}}$	$7.9 \cdot 10^{-5}$
$L_5$ in $\frac{L^*}{10^{51} \text{erg s}^{-1}}$	$9.8 \cdot 10^{-4}$
$\alpha_1$	1.2
$\alpha_2$	0.54
$\alpha_3$	-0.23
$\alpha_4$	-2.74
$D$	0.063
$P_{KS}$	0.507

68 KSONE in [18], finds the maximum distance,  $D$ , between the theoretical and the observed DF as well  
 69 the significance level,  $P_{KS}$ , see formulas 14.3.5 and 14.3.9 in [18]; values of  $P_{KS} \geq 0.1$  indicate that the  
 70 fit is acceptable, see Table 7 for the results.

71 In the case of the  $\Lambda$ CDM cosmology Figure 6 reports the lognormal DF, with parameters as in Table  
 72 7.

73 In the case of the  $\Lambda$ CDM cosmology, Figure 7 reports a comparison between the empirical distribution  
 74 and the lognormal PDF, and Figure 6 reports the lognormal DF, with parameters as in Table 7.

75 The case of the plasma and pseudo-Euclidean cosmologies are covered in Figs 8 and 9 respectively.

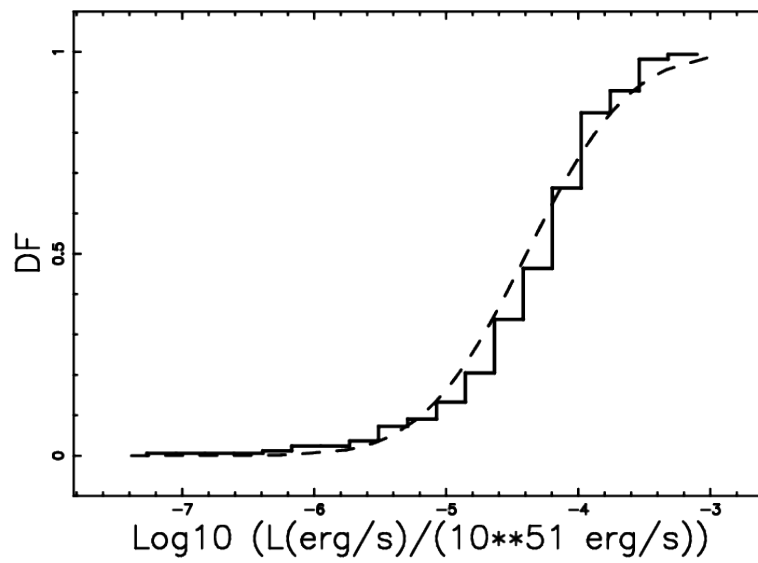


**Figure 6.** Observed DF (step-diagram) for GRB luminosity and superposition of the lognormal DF (line), case of the  $\Lambda$ CDM cosmology with parameters as in Table 7.

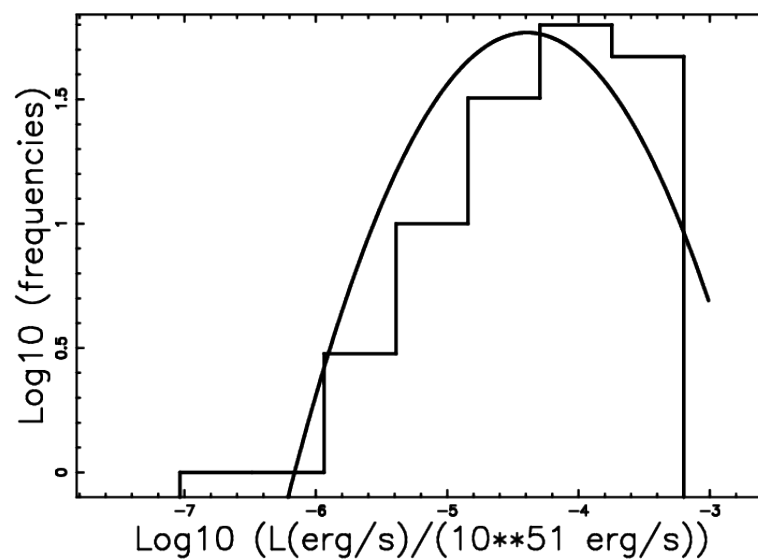


**Figure 7.** Log–Log histogram (step-diagram) of GRB luminosity and superposition of the lognormal PDF (line), case of the pseudo-Euclidean cosmology with parameters as in Table 7.

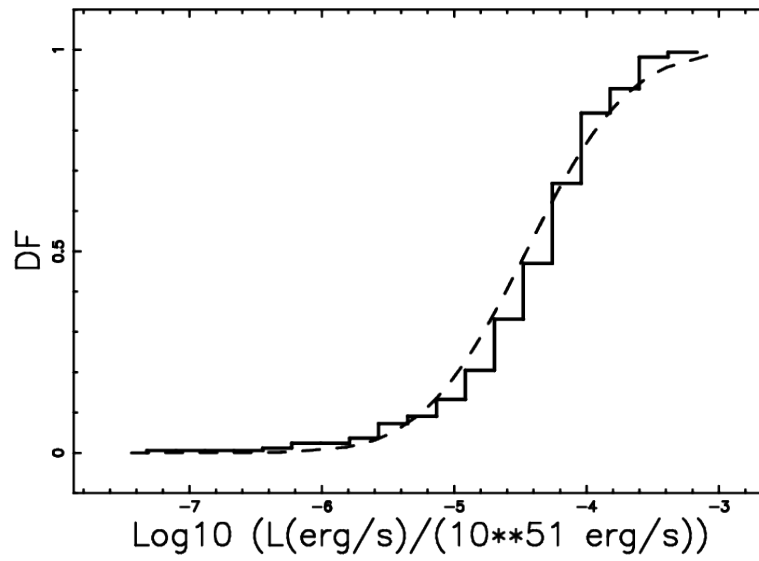


**Figure 8.** Observed DF (step-diagram) for GRB luminosity and superposition of the lognormal DF (line), case of the plasma cosmology with parameters as in Table 7.

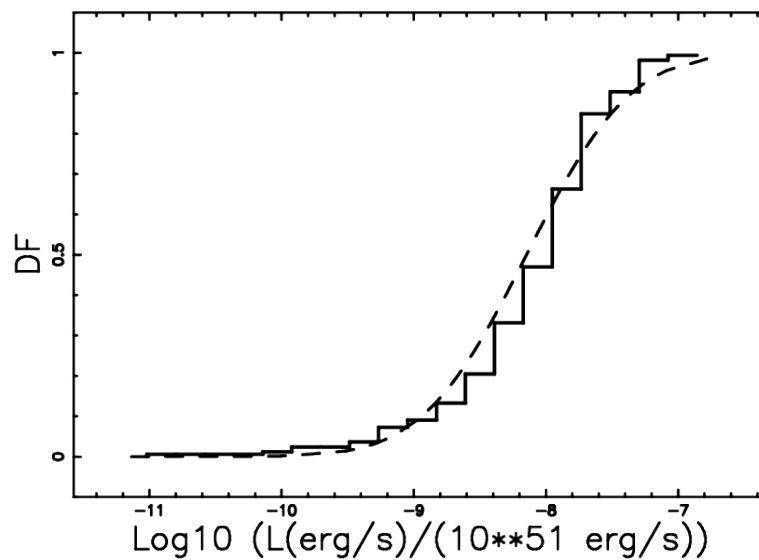


**Figure 9.** Observed DF (step-diagram) for GRB monochromatic luminosity, X-band (14–195 keV), and superposition of the lognormal DF (line), case of the pseudo-Euclidean cosmology with parameters as in Table 7.

**Table 7.** The 3 parameters of the LF as modeled by the lognormal distribution for  $z$  in  $[0, 0.02]$  with the Union 2.1 data and the two parameters of the K–S test  $D$  and  $P_{KS}$ . In the case of the plasma cosmology and the  $\Lambda$ CDM cosmology we used the luminosity as given by eqn (13) and eqn (8), respectively.

Parameter	Plasma cosmology	$\Lambda$ CDM cosmology
$\frac{L^*}{10^{51} \text{erg s}^{-1}}$	$3.516 \cdot 10^{-5}$	$4.055 \cdot 10^{-5}$
$\sigma$	1.42	1.42
$\frac{\Phi^*}{\text{Mpc}^{-3} \text{yr}^{-1}}$	$7.2524 \cdot 10^{-8}$	$1.025 \cdot 10^{-5}$
$D$	0.089	0.090
$P_{KS}$	0.131	0.127

**Table 8.** The 3 parameters of the LF, case of X-band (14–195 keV), as modeled by the lognormal distribution for  $z$  in  $[0, 0.02]$  with the Union 2.1 data and the two parameters of the K–S test,  $D$  and  $P_{KS}$ . In the case of the plasma cosmology and the pseudo-Euclidean cosmology, we used the luminosity as given by eqn (12) and eqn (16), respectively.

Parameter	Plasma cosmology	pseudo-Euclidean cosmology
$\frac{L^*}{10^{51} \text{erg s}^{-1}}$	$5.9 \cdot 10^{-9}$	$7.12 \cdot 10^{-9}$
$\sigma$	1.42	1.42
$\frac{\Phi^*}{\text{Mpc}^{-3} \text{yr}^{-1}}$	$1.01 \cdot 10^{-5}$	$9.88 \cdot 10^{-6}$
$D$	0.089	0.089
$P_{KS}$	0.13	0.129

### 76 3.3. The linear case

We assume that the flux,  $f$ , scales as  $f = \frac{L}{4\pi r^2}$ , according to eqn (15):

$$r = \frac{z c}{H_0} \quad , \quad (29)$$

and

$$z = \frac{r H_0}{c} \quad . \quad (30)$$

The relation between the two differentials  $dr$  and  $dz$  is

$$dr = \frac{c dz}{H_0} \quad . \quad (31)$$

The joint distribution in  $z$  and  $f$  for the number of galaxies is

$$\frac{dN}{d\Omega dz df} = \frac{1}{4\pi} \int_0^\infty 4\pi r^2 dr \Phi\left(\frac{L}{L^*}\right) \delta\left(z - \left(\frac{r H_0}{c}\right)\right) \delta\left(f - \frac{L}{4\pi r^2}\right) \quad , \quad (32)$$

where  $\delta$  is the Dirac delta function. We now introduce the critical value of  $z$ ,  $z_{crit}$ , which is

$$z_{crit}^2 = \frac{H_0^2 L^*}{4\pi f c^2} \quad . \quad (33)$$

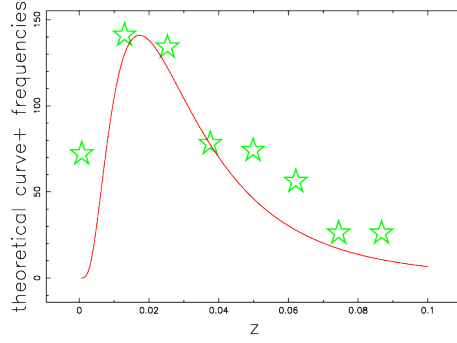


**Figure 10.** The GRBs of the SWIFT-BAT catalog with  $3.1 \frac{fW}{m^2} \leq f \leq 150.54 \frac{fW}{m^2}$ , which means  $\langle f \rangle = 76.82 \frac{fW}{m^2}$ , are organized in frequencies versus spectroscopic redshift (green stars). The redshift covers the range  $[0, 0.1]$ , the maximum frequency in the observed GRBs is at  $z = 0.019$ ,  $\chi^2 = 5925$  and the number of bins is 8. The full red line is the theoretical curve generated by  $\frac{dN}{d\Omega dz df}(z)$  as given by the application of the lognormal LF which is eqn (34) in the pseudo-Euclidean cosmology with parameters as in Table 7.

The evaluation of the integral over luminosities and distances gives

$$\frac{dN}{d\Omega dz df} = F(z; f, \Phi^*, L^*, \sigma) = \frac{z^2 c^3 \sqrt{2} e^{-\frac{1}{2} \frac{1}{\sigma^2} \left( \ln \left( \frac{z^2}{z_{crit}^2} \right) \right)^2} \Phi^*}{2 \sqrt{\pi} H_0^3 f \sigma}, \quad (34)$$

where  $d\Omega$ ,  $dz$  and  $df$  represent the differential of the solid angle, the redshift, and the flux, respectively, and  $\Phi^*$  is the normalization of the lognormal LF for GRB. The number of GRBs in  $z$  and  $f$  as given by the above formula has a maximum at  $z = z_{pos-max}$ , where

$$z_{pos-max} = e^{\frac{1}{2} \sigma^2} z_{crit}, \quad (35)$$

which can be re-expressed as

$$z_{pos-max} = \frac{e^{\frac{1}{2} \sigma^2} \sqrt{L^*} H_0}{2 \sqrt{\pi} \sqrt{f} c}. \quad (36)$$

Figure 10 reports the observed and theoretical number of GRBs with a given flux as a function of the redshift. The theoretical maximum as given by eqn (35) is at  $z = 0.017$ , with the parameters as in Table 7, against the observed  $z = 0.019$ . The theoretical mean redshift of GRBs with flux  $f$  can be deduced from eqn (34):

$$\langle z \rangle = \frac{\int_0^\infty z F(z; f, L^*, \Phi^*, \sigma) dz}{\int_0^\infty F(z; f, L^*, \Phi^*, \sigma) dz}. \quad (37)$$

77 The above integral does not have an analytical expression, and should be numerically evaluated. The  
 78 above formula with parameters as in Figure 10 gives a theoretical/numerical  $\langle z \rangle = 0.0368$  against the  
 79 observed  $\langle z \rangle = 0.0385$ . The quality of the fit in the number of GRBs with a given flux depends on the  
 80 chosen flux, the interval of the flux in which the frequencies are evaluated, and the number of histograms.  
 81 A larger number of available GRBs will presumably increase the goodness of the fit.

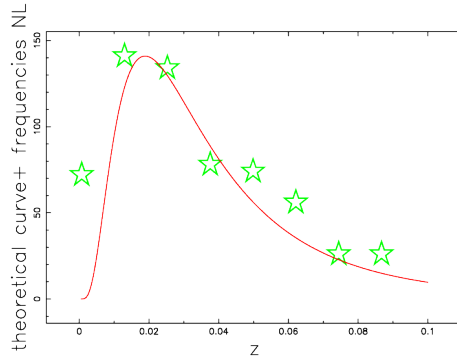


**Figure 11.** Frequencies of GRBs at a given flux as a function of the redshift, parameters as in Figure 10. The full red line is the theoretical curve generated by  $\frac{dN}{d\Omega dz df}(z)$  as given by the application of the lognormal LF which is eqn (41) in the plasma cosmology with parameters as in Table 8,  $\chi^2 = 6193$ .

### 82 3.4. The non-linear case

We assume that  $f = \frac{L}{4\pi r^2}$  and

$$z = e^{(H_0 r/c)} - 1 \quad , \quad (38)$$

where  $r$  is the distance; in our case,  $d$  is as represented by the non-linear eqn (11). The relation between  $dr$  and  $dz$  is

$$dr = \frac{cdz}{(z+1)H_0} \quad . \quad (39)$$

The joint distribution in  $z$  and  $f$  for the number of galaxies is

$$\frac{dN}{d\Omega dz df} = \frac{1}{4\pi} \int_0^\infty 4\pi r^2 dr \Phi\left(\frac{L}{L^*}\right) \delta\left(z - (e^{(H_0 r/c)} - 1)\right) \delta\left(f - \frac{L}{4\pi r^2}\right) \quad , \quad (40)$$

83 where  $\delta$  is the Dirac delta function.

The evaluations of the integral over luminosities and distances gives

$$\frac{dN}{d\Omega dz df} = \frac{(\ln(z+1))^2 c^3 \sqrt{2} e^{-\frac{1}{2} \frac{1}{\sigma^2} \left(\ln\left(\frac{(\ln(z+1))^2}{z_{crit}^2}\right)\right)^2} \Phi^*}{2 \sqrt{\pi} H_0^3 f \sigma (z+1)} \quad . \quad (41)$$

The above formula has a maximum at  $z = z_{pos-max}$ , where

$$z_{pos-max} = e^{4 \frac{W\left(\frac{1}{4} \sigma^2 z_{crit} e^{\frac{1}{2} \sigma^2}\right)}{\sigma^2}} - 1 \quad , \quad (42)$$

where  $W(x)$  is the Lambert  $W$  function, see [14]. The above maximum can be re-expressed as

$$z_{pos-max} = e^{4 \frac{1}{\sigma^2} W\left(\frac{1}{8} \frac{\sigma^2 \sqrt{L^*} H_0 e^{\frac{1}{2} \sigma^2}}{\sqrt{\pi} \sqrt{f} c}\right)} - 1 \quad . \quad (43)$$

84 Figure 11 reports the observed and theoretical number of GRBs with a given flux as a function of the  
 85 redshift. In the case of the plasma cosmology, the theoretical maximum as given by eqn (42) is at  
 86  $z = 0.0188$ , with the parameters as in Table 7, against the observed  $z = 0.019$ . The theoretical averaged  
 87 redshift of GRBs is  $\langle z \rangle = 0.041$  against the observed  $\langle z \rangle = 0.0385$ .

#### 88 4. The truncated lognormal distribution

89 This section derives the normalization and the mean for a truncated lognormal PDF. This truncated  
90 PDF fits the high redshift behaviour of the LF for GRBs.

##### 91 4.1. Basic equations

Let  $X$  be a random variable taking values  $x$  in the interval  $[x_l, x_u]$ ; the truncated lognormal (TL) PDF is

$$TL(x; m, \sigma, x_l, x_u) = \frac{\sqrt{2}e^{-\frac{1}{2}\frac{1}{\sigma^2}(\ln(\frac{x}{m}))^2}}{\sqrt{\pi}\sigma \left( -\operatorname{erf}\left(\frac{1}{2}\frac{\sqrt{2}}{\sigma}\ln\left(\frac{x_l}{m}\right)\right) + \operatorname{erf}\left(\frac{1}{2}\frac{\sqrt{2}}{\sigma}\ln\left(\frac{x_u}{m}\right)\right) \right)} x. \quad (44)$$

Its expected value is

$$E(m, \sigma, x_l, x_u) = \frac{e^{\frac{1}{2}\sigma^2} m \left( \operatorname{erf}\left(\frac{1}{2}\frac{\sqrt{2}(\sigma^2 + \ln(m) - \ln(x_l))}{\sigma}\right) - \operatorname{erf}\left(\frac{1}{2}\frac{\sqrt{2}(\sigma^2 + \ln(m) - \ln(x_u))}{\sigma}\right) \right)}{\operatorname{erf}\left(\frac{1}{2}\frac{\sqrt{2}(-\ln(x_l) + \ln(m))}{\sigma}\right) - \operatorname{erf}\left(\frac{1}{2}\frac{\sqrt{2}(-\ln(x_u) + \ln(m))}{\sigma}\right)}. \quad (45)$$

The distribution function is

$$DF(x; m, \sigma, x_l, x_u) = \frac{-\operatorname{erf}\left(\frac{1}{2}\frac{\sqrt{2}}{\sigma}\ln\left(\frac{x}{m}\right)\right) + \operatorname{erf}\left(\frac{1}{2}\frac{\sqrt{2}}{\sigma}\ln\left(\frac{x_l}{m}\right)\right)}{\operatorname{erf}\left(\frac{1}{2}\frac{\sqrt{2}}{\sigma}\ln\left(\frac{x_l}{m}\right)\right) - \operatorname{erf}\left(\frac{1}{2}\frac{\sqrt{2}}{\sigma}\ln\left(\frac{x_u}{m}\right)\right)}. \quad (46)$$

The four parameters which characterize the truncated lognormal distribution can be found with the maximum likelihood estimators (MLE) and by the evaluation of the minimum and maximum elements of the sample. The LF for GRB as given by the truncated lognormal,  $\Phi_T(L; L^*, \sigma, L_l, L_u)$ , is therefore

$$\Phi_T(L; L^*, \sigma, L_l, L_u) = \Phi^* TL(L; L^*, \sigma, L_l, L_u) \frac{\text{number}}{Mpc^3 yr}, \quad (47)$$

92 where  $L^*$  is the scale,  $L_l$  the lower bound in luminosity,  $L_u$  the upper bound in luminosity and  $\Phi^*$  is  
93 given by eqn (27).

##### 94 4.2. Applications at high $z$

95 The LF for GRBs as modeled by a truncated lognormal DF is reported in Figure 12 in the case of the  
96  $\Lambda$ CDM cosmology and in Figure 13 in the case of the plasma cosmology without a  $k(z)$  correction; the  
97 data is as in Table 9.

In order to model evolutionary effects, a variable upper bound in luminosity,  $L_u$ , has been introduced

$$L_u = 1.25(1+z)^2 10^{51} \frac{erg}{s}, \quad (48)$$

see eqn (7) in [5]; conversely the lower bound,  $L_l$  was already fixed by eqn (8). A second evolutionary correction is

$$\sigma = \sigma_0(1+z)^2, \quad (49)$$

98 where  $\sigma_0$  is the evaluation of  $\sigma$  at  $z \approx 0$ , see Table 9.

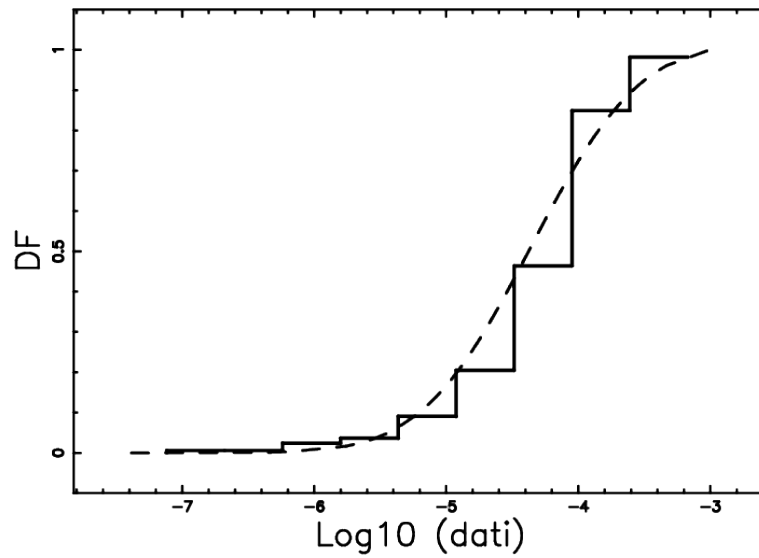


**Figure 12.** Observed DF (step-diagram) for GRB luminosity and superposition of the truncated lognormal DF (line), case of the  $\Lambda$ CDM cosmology with parameters as in Table 9.

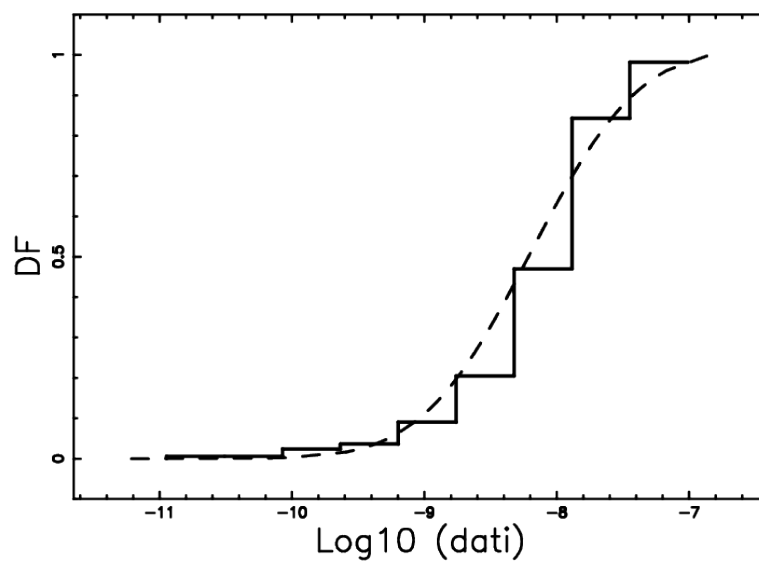


**Figure 13.** Observed DF (step-diagram) for GRB luminosity and superposition of the truncated lognormal DF (line), the case of the Plasma cosmology without  $k(z)$  correction with parameters as in Table 9.



**Table 9.** The 5 parameters of the LF as modeled by the truncated lognormal distribution for  $z$  in  $[0, 0.02]$  and the two parameters of the K–S test  $D$  and  $P_{KS}$ . We analysed the case of the  $\Lambda$ CDM cosmology where the luminosity is given by eqn (8) in the second column and the case of the plasma cosmology, the case of the X-band (14–195 keV) without  $k(z)$  correction, where the luminosity is given by eqn (12), third column.

Parameter	$\Lambda$ CDM cosmology	Plasma cosmology
$\frac{L_l}{10^{51} \text{erg s}^{-1}}$	$4.11 \cdot 10^{-8}$	$6.11 \cdot 10^{-12}$
$\frac{L_u}{10^{51} \text{erg s}^{-1}}$	$9.8 \cdot 10^{-4}$	$1.42 \cdot 10^{-7}$
$\frac{L^*}{10^{51} \text{erg s}^{-1}}$	$4.05 \cdot 10^{-5}$	$5.9 \cdot 10^{-9}$
$\sigma$	1.42	1.42
$\frac{\Phi^*}{\text{Mpc}^{-3} \text{yr}^{-1}}$	$1.02 \cdot 10^{-5}$	$1.01 \cdot 10^{-5}$
$D$	0.084	0.084
$P_{KS}$	0.177	0.18

99 Figure 14 reports a comparison between the theoretical average luminosity and the observed average  
100 luminosity for the  $\Lambda$ CDM cosmology.

In the case of the plasma cosmology, the variable upper bound in luminosity,  $L_u$ , is

$$L_u = 1.25(1 + z)^2 10^{47} \frac{\text{erg}}{\text{s}}, \quad (50)$$

101 and Figure 15 reports a comparison between the theoretical average luminosity and the observed average  
102 luminosity for the plasma cosmology.

## 103 5. Conclusions

### 104 Luminosity

105 The evaluation of the luminosity is connected with the evaluation of the luminosity distance, which is  
106 different for every adopted cosmology: the  $\Lambda$ CDM and plasma cosmologies cover the range in  $z$   $[0 - 4]$   
107 and the pseudo-Euclidean cosmology covers the limited range in  $z$ ,  $[0 - 0.15]$ .

108 An application of a correction for the luminosity over all the  $\gamma$  range which is  $[1 \text{ keV} - 10^4 \text{ keV}]$   
109 allows speaking of the extended luminosity of a GRB; in the case of  $\Lambda$ CDM, see eqn (8), which depends  
110 on the three observable parameters  $flux_{wm2}$ ,  $z$  and  $\gamma$ . An analytical formula for the luminosity in  
111  $\Lambda$ CDM without corrections is given as a function of the two observable parameters  $flux_{wm2}$  and  $z$ ,  
112 see eqn (6), which can be tested on the SWIFT-BAT catalog of [1].

### 113 Lognormal luminosity function

114 We analysed the widely used lognormal PDF as a LF for GRBs, see Section 3.2. We derived an  
115 expression for the maximum in the number of GRBs for a given flux, which is eqn (35) in the linear case  
116 (pseudo-Euclidean universe), see also Figure 10, and eqn (42) in the non-linear case (plasma cosmology),  
117 see also Figure 11.

### 118 Four broken power law luminosity function

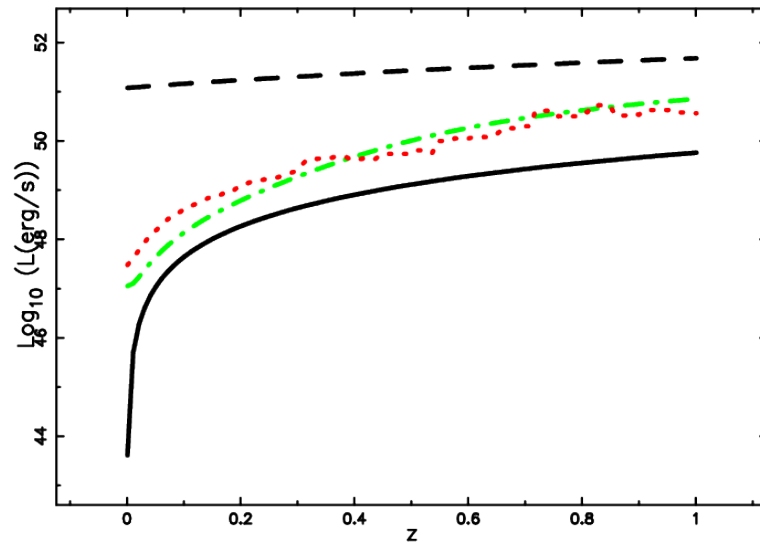


**Figure 14.** Average observed luminosity in the  $\Lambda$ CDM cosmology versus redshift for 784 GRB (red points), theoretical average luminosity for truncated lognormal LF as given by eqn (45) (dot-dash-dot green line), theoretical curve for the lowest luminosity at a given redshift, see eqn (12) (full black line) and the empirical curve for the highest luminosity at a given redshift (dashed black line), see eqn (50).

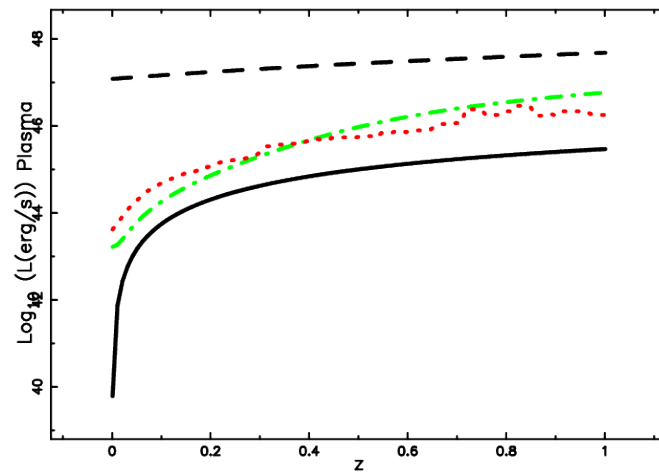


**Figure 15.** Average observed luminosity in the Plasma cosmology without  $k(z)$  correction versus redshift for 784 GRB (red points), theoretical average luminosity for truncated lognormal LF as given by eqn (45) (dot-dash-dot green line), theoretical curve for the lowest luminosity at a given redshift, see eqn (8) (full black line) and the empirical curve for the highest luminosity at a given redshift (dashed black line), see eqn (50).

119 The four broken power law PDF gives the best statistical results for the LF of GRBs, see Table 6. The  
 120 weak point of this LF is in the number of parameters, which is 9, against the 4 of the truncated lognormal  
 121 LF or 2 of the lognormal LF.

### 122 **Maximum in flux**

123 The maximum in the joint distribution in redshift and energy flux density is here modeled in the case  
 124 of a pseudo-Euclidean universe adopting a standard technique originally developed for galaxies, see  
 125 formula (5.132) in [19] and our formula (34). In the case of the plasma cosmology, the maximum has  
 126 been found by analogy, see our formula (34). In the case of the  $\Lambda$ CDM cosmology, the redshift as a  
 127 function of the luminosity has a complex behaviour, see formula (66) in [10], and the analysis has been  
 128 postponed to future research. The above complexity has been considered in an example of a simpler  
 129 plasma cosmology rather than in the  $\Lambda$ CDM cosmology.

### 130 **Evolutionary effects**

131 The LF for GRBs at high  $z$  is well modeled by a truncated lognormal PDF, see Section 4.1. The  
 132 lower bound for the luminosity is fixed by the decrease in the range of observable luminosities and the  
 133 higher bound by a standard assumption, see eqn (48). A further refinement of the truncated lognormal  
 134 model for the GRBs at high  $z$  is obtained by introducing a cosmological correction for  $\sigma$ , see eqn (49),  
 135 see Figure 12 for the case of the  $\Lambda$ CDM cosmology and Figure 15 for the case of the plasma cosmology.  
 136 In other words, the  $\Lambda$ CDM cosmology and the plasma cosmology are indistinguishable in the range of  
 137 redshifts here analysed,  $0 \leq z \leq 4$ .

## 138 **References**

- 139 1. Baumgartner, W.H.; Tueller, J.; Markwardt, C.B.; Skinner, G.K.; Barthelmy, S.; Mushotzky,  
 140 R.F.; Evans, P.A.; Gehrels, N. The 70 Month Swift-BAT All-sky Hard X-Ray Survey. *ApJS*  
 141 **2013**, *207*, 19, [[arXiv:astro-ph.HE/1212.3336](https://arxiv.org/abs/1212.3336)].
- 142 2. McBreen, B.; Hurley, K.J.; Long, R.; Metcalfe, L. Lognormal Distributions in Gamma-Ray  
 143 Bursts and Cosmic Lightning. *MNRAS* **1994**, *271*, 662.
- 144 3. Ioka, K.; Nakamura, T. A Possible Origin of Lognormal Distributions in Gamma-Ray Bursts.  
 145 *ApJ* **2002**, *570*, L21–L24, [[astro-ph/0202053](https://arxiv.org/abs/astro-ph/0202053)].
- 146 4. Zaninetti, L. Relativistic Scaling Laws for the Light Curve in Supernovae. *Applied Physics*  
 147 *Research* **2015**, *7*, 48–59.
- 148 5. Tan, W.W.; Cao, X.F.; Yu, Y.W. Determining the Luminosity Function of Swift Long  
 149 Gamma-Ray Bursts with Pseudo-redshifts. *ApJ* **2013**, *772*, L8, [[arXiv:astro-ph.HE/1306.2681](https://arxiv.org/abs/astro-ph.HE/1306.2681)].
- 150 6. Zaninetti, L. Pade Approximant and Minimax Rational Approximation in Standard Cosmology.  
 151 *Galaxies* **2016**, *4*, 4–24.
- 152 7. Etherington, I.M.H. On the Definition of Distance in General Relativity. *Philosophical Magazine*  
 153 **1933**, *15*.
- 154 8. Brynjolfsson, A. Redshift of photons penetrating a hot plasma. *arXiv:astro-ph/0401420* **2004**.
- 155 9. Ashmore, L. Recoil Between Photons and Electrons Leading to the Hubble Constant and CMB.  
 156 *Galilean Electrodynamics* **2006**, *17*, 53.
- 157 10. Zaninetti, L. On the Number of Galaxies at High Redshift. *Galaxies* **2015**, *3*, 129–155.

- 158 11. Ashmore, L. A Relationship between Dispersion Measure and Redshift Derived in Terms of New  
159 Tired Light. *Journal of High Energy Physics, Gravitation and Cosmology* **2016**, 2, 512–530.
- 160 12. Evans, M.; Hastings, N.; Peacock, B. *Statistical Distributions - third edition*; John Wiley & Sons  
161 Inc: New York, 2000.
- 162 13. Johnson, N.L.; Kotz, S.; Balakrishnan, N. *Continuous univariate distributions. Vol. 1. 2nd ed.*;  
163 Wiley : New York, 1994.
- 164 14. Olver, F.W.J.e.; Lozier, D.W.e.; Boisvert, R.F.e.; Clark, C.W.e. *NIST handbook of mathematical*  
165 *functions.*; Cambridge University Press. : Cambridge, 2010.
- 166 15. Kolmogoroff, A. Confidence Limits for an Unknown Distribution Function. *The Annals of*  
167 *Mathematical Statistics* **1941**, 12, 461–463.
- 168 16. Smirnov, N. Table for Estimating the Goodness of Fit of Empirical Distributions. *The Annals of*  
169 *Mathematical Statistics* **1948**, 19, 279–281.
- 170 17. Massey, Frank J., J. The Kolmogorov-Smirnov Test for Goodness of Fit. *Journal of the American*  
171 *Statistical Association* **1951**, 46, 68–78.
- 172 18. Press, W.H.; Teukolsky, S.A.; Vetterling, W.T.; Flannery, B.P. *Numerical Recipes in FORTRAN.*  
173 *The Art of Scientific Computing*; Cambridge University Press: Cambridge, UK, 1992.
- 174 19. Peebles, P.J.E. *Principles of Physical Cosmology*; Princeton University Press: Princeton, N.J.,  
175 1993.

176 © April 24, 2022 by the author; submitted to *Galaxies* for possible open access  
177 publication under the terms and conditions of the Creative Commons Attribution license  
178 <http://creativecommons.org/licenses/by/4.0/>.